Semiconductors, 2022, Vol. 56, No. 6

Influence of low temperature on the electrophysical and noise characteristics of UV LEDs based on InGaN/GaN quantum well structures

© A.M. Ivanov, A.V. Klochkov

Ioffe Institute,
194021 St. Petersburg, Russia

E-mail: alexandr.ivanov@mail.ioffe.ru

Received February 20, 2022
Revised March 24, 2022
Accepted March 24, 2022

Comparison of optical power, external quantum efficiency in InGaN/GaN UV LEDs at room temperature and liquid nitrogen temperature is carried out. The spectral densities of the current low-frequency noise have been investigated. The mechanisms of carrier transport, the formation of low-frequency noise, and the dependences of the rates of radiative and nonradiative recombination at room and nitrogen temperatures are considered.

Keywords: External quantum efficiency, low-frequency noise, carrier transport, defect tunneling.

DOI: 10.21883/SC.2022.06.53546.9817

1. Introduction

The present-day production volume of ultraviolet (UV) light-emitting diodes (and lasers) based on InGaN/GaN and AlGaN/GaN is significantly increasing. This is related to the wide application areas of light-emitting devices of the given range, inaccessible for semiconductor sources of visible light. UV light-emitting diodes are used in industry and dentistry to accelerate solidification processes, in forensic science, banking business, plant growing, and, what is very important, in medicine, sanitary science, cosmetic medicine. Water sterilizing, detection of biological agents, covert communication and solid-state lighting [1] use optoelectronic devices of the given radiation range.

Research aimed at studying the physical mechanisms and improvement of electrophysical characteristics, reliability and service life in optoelectronic devices of the given radiation range is of undeniable interest and is widely discussed in modern publications. One of less-studied research areas is the behavior of light-emitting diodes under low temperatures.

A drop of luminescence intensity and external quantum efficiency with temperature rise was described in several papers in the ranges: from 280 to 340 [1], from 300 to 500 [2], from 290 to 360 K [3]. In this respect, research of radiating [4,5] and noise characteristics [6] of light-emitting diodes at low temperatures is promising since they can be used at negative ambient temperatures (in freezing chambers). Temperature decrease increases the luminous flux, reduces the LED degradation rate, reduces the semiconductor diode noise density. Distribution of carriers in the phase space for radiative recombination is improved. The effect of phase space fill makes a considerable contribution to the change of temperature-dependent coefficients of radiative and nonradiative recombination [2].

Research of noise density makes it possible to improve the device manufacture and engineering processes, allows for prediction of device service life [7], since noise characteristics are sensitive to LED degradation processes.

This paper describes a comparative research of UV LEDs at room temperature and liquid nitrogen temperature. The paper is aimed at checking device operability under a low temperature and the possibility to improve their characteristics at low temperatures different from the room one. Recombination processes, carrier transport and noise generation processes are discussed.

2. Experimental procedure

The experiments were conducted on commercial UV (UV-A) LEDs with InGaN/GaN quantum wells manufactured by Betlux (BL-L522VC having the peak radiation energy $h\nu_{\mathrm{QW}} = 3.06\,\mathrm{eV}$ or the radiation wavelength of $\lambda = 405\,\mathrm{nm}$, luminous intensity — 180 mcd). The LED active area was $\sim 10^{-3}\,\mathrm{cm}^2$, rated current $I = 20\,\mathrm{mA}$.

The light-emitting diode and the measuring photodiode were located at a fixed distance. A FD-7K silicon photodiode was used for relative changes of radiation efficiency and energy. A SCH300 digital ammeter was used to measure photo-induced current in the short-circuit mode. A GPS-4303 direct current power source and high-precision Agilent 34401A multivoltmeter were also used in the experiments.

Voltage fluctuations on resistance $R = 100\,\mathrm{Ohm}$ in time were recorded by means of an analog-to-digital converter. The researched frequency band was 10 Hz−7.3 kHz. Noise power was determined in four bands with the center frequencies of 20, 70, 270 and 1000 Hz. For more detail about determination of density of low-frequency current noise and its spectral dependence by means of a semi-automatic unit see paper [8]. Current, photo-induced current and density of low-frequency current noise were measured at room temperature ($T = 295\,\mathrm{K}$) and nitrogen temperature ($T = 77.4\,\mathrm{K}$).

3. Experimental results

Figure 1, *a* shows the results of measurement of optical power (photodiode current) vs. forward-bias current I. At $T = 295$ K the photoinduced current dependence in conventional $I_{ph} \propto I$. At $T = 77.4$ K the dependence has several peculiarities: a) a considerably lower threshold current $I_{th} = 1.0\,\mu$A; b) at $1 \leq I \leq 30\,\mu$A and at $1 \leq I \leq 20$ mA $I_{ph} \propto I$. At intermediate current values $30\,\mu\text{A} \leq I \leq 0.6$ mA $I_{ph} \propto I^{0.5}$, the photoinduced current dependence at low temperature first exceeds the photoinduced current at room temperature, and drops below it after the area $I_{ph} \propto I^{0.5}$.

Figure 1, *b* shows the dependences of external quantum efficiency on current $\eta(I)$. The dependence at $T = 295$ K has the conventional typical form with a slight drop at currents $I > 10$ mA. Efficiency at liquid nitrogen temperature: a) in the maximum it is 2 times greater than the efficiency at room temperature; b) the most abrupt drop is observed for the current area which corresponds to the dependence $I_{ph} \propto I^{0.5}$. Efficiency increase at milliampere currents corresponds to saturation and beginning of efficiency decrease at room temperature. The dependences were normalized to the maximum value of η at $T = 77.4$ K.

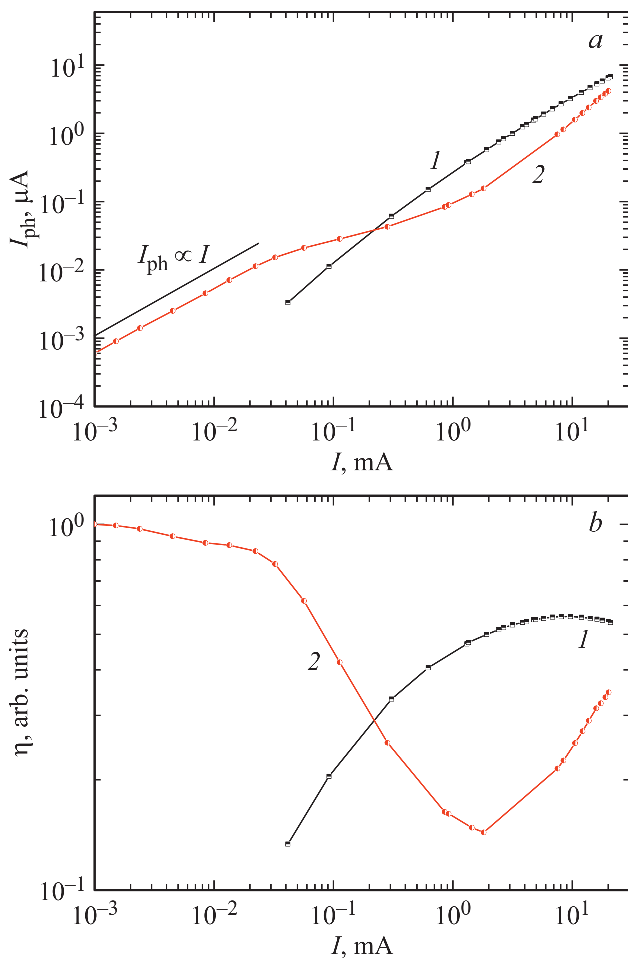

Figure 1. Dependences of photoinduced current (a) and external quantum efficiency (b) on forward-bias current for UV LED at T, K: *1* — 295, *2* — 77.4.

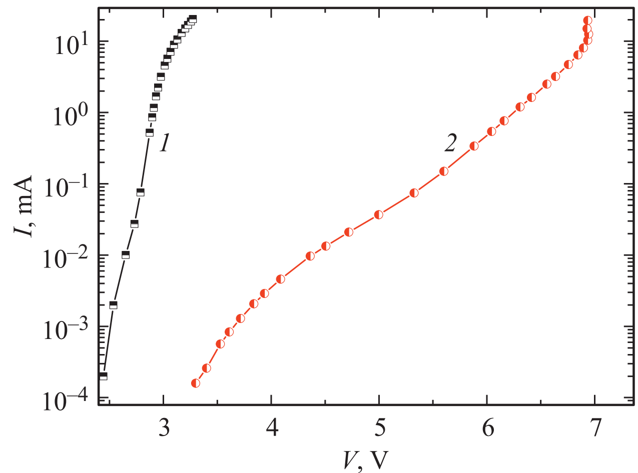

Figure 2. Dependences of current on voltage $I(V)$ at T, K: *1* — 295, *2* — 77.4.

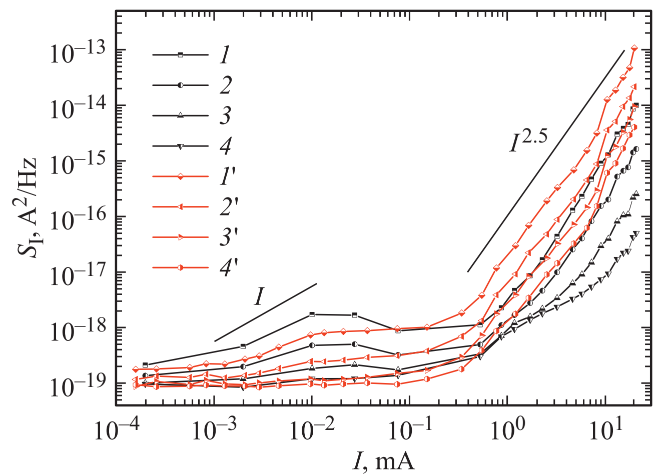

Figure 3. Dependences of current noise spectral density for different analysis frequencies at T, K: *1, 2, 3, 4* — 295, *1′, 2′, 3′, 4′* — 77.4. Analysis frequency, f, Hz: *1, 1′* — 20, *2, 2′* — 70, *3, 3′* — 270, *4, 4′* — 1000.

The dependences of flowing current on forward bias on the studied LEDs at $T = 295$ and 77.4 K are shown in Fig. 2. The current-voltage characteristic at room temperature is conventional. When temperature decreases to $T = 77.4$ K, the dependence shifts towards higher voltages.

The measured current-voltage dependences (Fig. 2) were used to determine the estimated current dependences on voltage on the $p{-}n$-transition $I(V_I)$. $V_I = V - Ir$, where r is series resistance (14 Ohm). The obtained dependences were approximated by the exponential function $I = I_0 \exp(qV_I/n_I(V_I)kT)$, where q — elementary charge, kT — thermal energy, $n_I(V_I)$ — ideality factor which characterizes the current passage specificity, calculated as $n_I(I) = (q/kT)/(d\ln I/dV_I)$.

Figure 3 shows the dependences of spectral density of low-frequency current noise on current at two temperatures

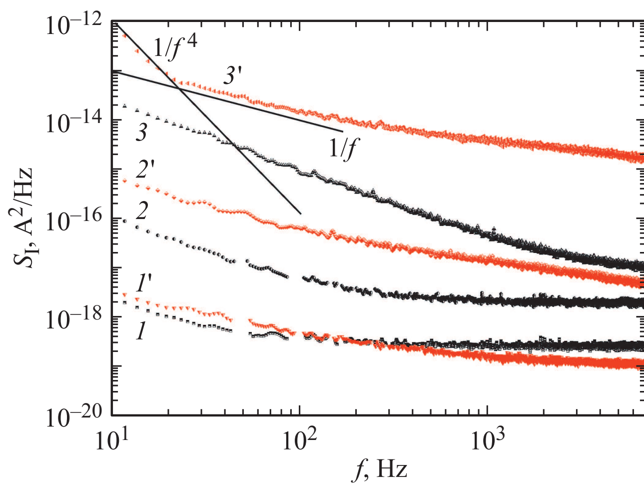

Figure 4. Frequency dependences of current noise spectral density at T, K: *1,2,3* — 295, *1′, 2′, 3′* — 77.4. At I, mA: *1* — 0.53, *1′* — 0.34, *2* — 3.2, *2′* — 3.3, *3* — 21.0, *3′* — 20.0.

for four analysis frequencies. Each frequency is characterized by an intersection point, after which the dependence of noise density at liquid nitrogen temperature increases sharply and is eventually by an order or more higher than the corresponding dependence for room temperature. Current noise density on these areas at $T = 77.4$ K is $S_I \propto I^{2.5}$.

A comparison of the frequency dependences of spectral density of low-frequency current noise at two temperatures is shown in Fig. 4. With milliampere currents, the observed noise density is considerably higher at $T = 77.4$ K than at $T = 295$ K. The dependences at both temperatures are close to $S_I \propto 1/f^\alpha$ ($\alpha \geq 1$) noise. Dependence at nitrogen temperature and $I = 20$ mA sharply increases only at the lowest frequency ($S_I \propto 1/f^4$).

4. Discussion

The fact that external quantum efficiency at low temperatures exceeds efficiency at room temperature (in our case, UV LEDs at $I \leq 0.2$ mA) is explained by a) decrease of nonradiative recombination rate; b) increase of radiative recombination due to better overlap of the electron and hole wave functions (radiative recombination coefficient depends on temperature in inverse proportion to $T^{3/2}$ [9]); c) decrease of tunnel leakage of carriers from a quantum well (QW) through the bulk charge region [10,11]; d) at $T < 80$ K the transfer of some carriers into quantum wells is ballistic or quasiballistic [5]. This improves the transport of carriers to active zones.

The area of slower increase of photoinduced current at nitrogen temperature corresponds to the area of a sharp decrease of quantum efficiency, and, as distinct from the data in [12], it becomes significantly lower than the efficiency at $T = 295$ K. Paper [12] described a monotonous rise of efficiency with temperature decrease (but not lower than $T = 160$ K) in the current range under study.

According to the ABC model (see, for instance, [13]), for internal quantum efficiency

$$\eta_{\text{int}} = \frac{Bn^2}{An + Bn^2 + Cn^3},$$

where A, B, C — coefficients of Shockley–Read–Hall (SRH) nonradiative recombination, radiative recombination and nonradiative Auger recombination respectively; n — carrier concentration. A fourth term $F(n)$ is added to the denominator to take into account the charge carrier outflow from a quantum well [14]. The calculated dependences: a) of A, B, C coefficients on temperature are given in [2], b) recombination rate on current for different mechanisms are given in [15]. B and C increase as temperature decreases. An additional factor is carrier concentration which increases with current increase. B decreases with increase of n, while A increases. This can explain the descending section of quantum efficiency at $T = 77.4$ K (see Fig. 1, *b*). Subsequent efficiency increase ($I > 2$ mA) is due to the fact that radiative recombination rate at such currents prevails over nonradiative recombination rates [15].

An insignificant increase of current noise density ($S_I \propto I$) at the frequencies of 20 and 70 Hz on the initial area ($I \leq 10\,\mu$A) of the current dependence (Fig. 3) does not allow for making a conclusion on presence of a fractal-percolation system in the samples [6]. A significant increase of noise at $I > 0.5$ mA for both temperatures ($S_I \propto I^{2.5}$) can be explained by rearrangement or formation of new defects [16,17], flowing high-density current due to a non-uniform distribution of the carrier stream along the LED structure cross-section [6,16]. Such changes in the defect spectrum can be due to energy emitted under nonradiative recombination, i.e. SRH and Auger recombination, since the emitted energy is close to the band gap [15,18].

Figure 4 confirms an increase of low-frequency noise density at $T = 77.4$ K as compared to room temperature for the milliampere current range (curves *2, 2′, 3, 3′*). These dependences at a higher current have a sharper slope ($\propto 1/f^\alpha$) in the low-frequency part, $\alpha \geq 1$. Special attention should be paid to the dependence *3′* ($I = 20$ mA $T = 77.4$ K), for which at the lowest frequencies ($f < 30$ Hz) $\alpha \approx 4$; at 30 Hz $< f <$ 1000 Hz $\alpha \approx 2$, i.e. it is Lorentzian. An increase of noise density with increase of the current magnitude at $>$ 3000 Hz may mean an increase of Gaussian noise. Noise with a „white“ spectrum at these frequencies is associated with shot noise due to incidental photon radiation [7].

The observed frequency dependences of noise density with $\alpha \geq 2$ presuppose adding-up of several kinds of noise having a different nature. Such noise can be flicker noise, generation-recombination noise (having $S_I \propto I^2$ [19]), telegraph noise and noise related to defect tunneling.

The role of defects in GaN-based nitride nanostructures is ambiguous. A high density of defects with deep levels in LED structures with InGaN/GaN quantum wells ensures the trap-assisted tunneling of charge carriers (TAT, the model is outlined in [20]) through potential barriers to the active

region. This kind of carrier transport becomes predominant with temperature decrease [21,22]. The duality of defect occurrence in the space charge region (SCR) consists in involvement in SRH recombination and provision of carrier transport.

As distinct from resonant tunneling, the critical factor in case of the TAT mechanism is the distance between impurities and defects, but not the width of space charge region (SCR). This mechanism is implemented not only in InGaN/GaN light-emitting diodes, but, as shown earlier, also in $p-i-n$-diodes on amorphous silicon (a-Si:H) [23]. Thus, we can speak of possible hopping transport where carriers tunnel to distances of $3-5\,\mu$m. Tunneling takes place across zone ends and defects, density of which is the minimum directly near a QW.

A model of the mechanism of low-frequency noise generation based on fluctuation of center occupation under horizontal energy transitions [8], despite the physical difference, is described using the same mathematical representations (Lorentzian noise spectrum) as generation-recombination noise [24], related to vertical energy transitions between centers and unoccupied bands. Fluctuations are determined by a random distribution of centers in depth of the barriers' SCR and an exponential dependence of hopping frequency on distance between centers, determined by density of states at the tunneling level [25,26], which causes fluctuations of center filling and current noise.

A possible defect formation and a change of the spectrum of deep centers in the band gap of InGaN/GaN structures with quantum wells at $I > 0.5$ mA manifests itself in an increased defect-assisted carrier tunneling and fluctuation of hopping resistance. The non-uniform distribution of local hopping resistance causes modulation of through current and increase of low-frequency noise.

The calculated value of ideality factor n_I (from the current-voltage dependence at $T = 295$ K, see Fig. 2) does not exceed 3, in the range of $100\,\mu$A-1 mA it decreases to 1.4, while at $I > 10$ mA it drops to 1. It means that the fraction of defect-assisted tunneling current decreases as forward bias increases, while the fraction of over-barrier carrier injection in QW increases, radiative recombination in QW increases. The magnitude of n_I at liquid nitrogen temperature in almost the entire range of measured currents is $n_I > 7$ and defect tunneling prevails in the current, recombination in barriers reduces efficiency as compared to room temperature. Accordingly, generation-recombination noise prevails in Lorentzian noise at room temperature, while the fraction of tunneling resistance noise is significant at $T = 77.4$ K.

5. Conclusion

1) The performed testing has shown operability of UV LEDs under low temperatures ($T = 77.4$ K).

2) A considerable increase of current noise density at $T = 77.4$ K presupposes less reliable operation of InGaN/GaN LEDs in such conditions. Defect tunneling plays an important role in the carrier transport.

3) Despite the increase of external quantum efficiency at low currents ($< 100\,\mu$A) at liquid nitrogen temperature, efficiency decreased at nominal currents. Additional research is required to determine the boundary temperature of positive and negative changes under cooling.

Thus, the performed analysis of characteristics of commercial UV LEDs based on InGaN/GaN structures with quantum wells at room temperature and liquid nitrogen temperature has revealed a significant drop of external quantum efficiency and an increase of low-frequency current noise density at nominal currents and $T = 77.4$ K. The possible physical mechanisms to explain the observed effects are presented. At $T = 77.4$ K, the significance of defect tunneling in carrier transport increases; the spectrum of defects can change due to energy released during recombination. The current dependences of efficiency and noise density at intermediate temperatures are of doubtless interest.

Conflict of interest

The authors declare that they have no conflict of interest.

References

[1] Z. Peng, W. Guo, T. Wu, Z. Guo, Y. Lu, Y. Zheng, Y. Lin, Z. Chen. IEEE Photonics J., **12** (1), 8200108 (2020).

[2] P. Tian, J.J.D. McKendry, J. Herrnsdorf, S. Watson, R. Ferreira, I.M. Watson, E. Gu, A.E. Kelly, M.D. Dawson. Appl. Phys. Lett., **105**, 171107 (2014).

[3] D. Monti, M. Meneghini, C. De Santi, G. Meneghesso, E. Zanoni. IEEE Trans. Dev. Mater. Reliab., **16** (2), 213 (2016).

[4] S. Marcinkevicius, R. Yapparov, L.Y. Kuritzky, Y-R. Wu, S. Nakamura, J.S. Speck. Phys. Rev. B, **101**, 075305 (2020).

[5] D.S. Arteev, A.V. Sakharov, A.E. Nikolaev, W.V. Lundin, A.F. Tsatsulnikov. J. Luminesc., **234**, 117957 (2021).

[6] V.V. Emtsev, E.V. Gushchina, V.N. Petrov, N.A. Tal'nishnih, A.E. Chernyakov, E.I. Shabunina, N.M. Shmidt, A.S. Usikov, A.P. Kartashova, A.A. Zybin, V.V. Kozlovski, M.F. Kudoyarov, A.V. Saharov, A.G. Oganesyan, D.S. Poloskin and V.V. Lundin, Semicond., **52** (7), 942 (2018).

[7] B. Šaulys, J. Matukas, V. Palenskis, S. Pralgauskaite, G. Kulikauskas. Acta Phys. Polon. A, **119** (4), 514 (2011).

[8] N.I. Bochkareva, A.M. Ivanov, A.V. Klochkov, Y.G. Shreter, Semicond., **53** (1), 99 (2019).

[9] F. Shubert. *Svetodiody* (M., Fizmatlit, 2008) p. 77 (in Russian).

[10] N.I. Bochkareva, V.V. Voronenkov, R.I. Gorbunov, A.S. Zubrilov, Y.S. Lelikov, F.E. Latyshev, Y.T. Rebane, A.I. Tsyuk, Y.G. Shreter, Semicond., **44** (6), 794 (2010).

[11] N.I. Bochkareva, V.V. Voronenkov, R.I. Gorbunov, F.E. Latyshev, Y.S. Lelikov, Y.T. Rebane, A.I. Tsyuk, Y.G. Shreter, Semicond., **47** (1), 127 (2013).

[12] A.S. Pavluchenko, I.V. Rozhansky, D.A. Zakheim, Semicond., **43** (10), 1351 (2009).

[13] S.Yu. Karpov. Optical Quant. Electron., **47** (6), 1293 (2015).

[14] Q. Lv, J. Gao, X. Tao, J. Zhang, C. Mo, X. Wang, C. Zheng, J. Liu. J. Luminesc., **222**, 117186 (2020).

[15] N. Renso, C. De Santi, A. Caria, F. Dalla Torre, L. Zecchin, G. Meneghesso, E. Zanoni, M. Meneghini. J. Appl. Phys., **127**, 185701 (2020).
[16] A.E. Chernyakov, M.E. Levinshtein, N.A. Talnishnikh, E.I. Shabunina, N.M. Shmidt. J. Cryst. Growth, **401**, 302 (2014).
[17] G.P. Zhigalsky. UFN, **173** (5), 465 (2003) (in Russian).
[18] I.N. Yassievich. Semicond. Sci. Technol., **9**, 1433 (1994).
[19] I-H. Lee, A.Y. Polyakov, S-M. Hwang, N.M. Shmidt, E.I. Shabunina, N.A. Tal'nishnih, N.B. Smirnov, I.V. Shchemerov, R.A. Zinovyev, S.A. Tarelkin, S.J. Pearton. Appl. Phys. Lett., **111**, 062103 (2017).
[20] M. Auf der Maur, B. Galler, I. Pietzonka, M. Strassburg, H. Lugauer, A. Di Carlo. Appl. Phys. Lett., **105**, 133504 (2014).
[21] R.J. Molnar, T. Lei, T.D. Moustakas. Appl. Phys. Lett., **62** (1), 72 (1993).
[22] N.I. Bochkareva, Yu.G. Shreter. FTT, **64** (3), 371 (2022) (in Russian).
[23] D. Han, K. Wang, C. Yeh, L. Yang, X. Deng, B. Von Roedern. Phys. Rev. B, **55** (23), 15619 (1997).
[24] N.V. Dyakonova, M.E. Levinshtein, S.L. Rumyantsev. FTP, **25** (12), 2065 (1991) (in Russian).
[25] N.I. Bochkareva, Y.T. Rebane, Y.G. Shreter, Semicond., **49** (12), 1665 (2015).
[26] N.I. Bochkareva, A.M. Ivanov, A.V. Klochkov, Y.G. Shreter. J. Phys.: Conf. Ser., **1697**, 012203 (2020).